RSC Advances

PAPER

Functionalized porous microparticles of nanofibrillated cellulose for biomimetic hierarchically structured superhydrophobic surfaces†

Henrikki Mertaniemi,[a] Antti Laukkanen,[b] Jan-Erik Teirfolk,[b] Olli Ikkala[a] and Robin H. A. Ras*[a]

Nanofibrillated cellulose (NFC, also called microfibrillated cellulose and native cellulose nanofibers) is an attractive sustainable nanofibrillar material to template functionalities. It allows the modification of wetting properties, but so far surfaces with NFC have suffered from high adhesion of water droplets, even when the contact angles have been large. Here we show that spray-dried NFC leads to hierarchical surface roughness, closely resembling that of lotus leaves, due to the microparticles and their porosity at a considerably smaller length scale. We present the first report on superhydrophobic surfaces from NFC with contact angle hysteresis of only a few degrees upon surface modification. The shown process to achieve the hierarchies is particularly straightforward involving airbrushing of solvent-based NFC onto the surface, followed by quick drying, and a chemical modification performed either before or after the airbrushing, with essentially similar results. The NFC microparticles also enable the formation of liquid marbles. The presented method is technically feasible, as cellulose is an economic, abundant material from nature and the spraying processes are scalable. The shown approach could allow further functionalities, such as self-cleaning and water droplet manipulation.

Introduction

The extraordinary wetting properties of plants, especially of the leaves of lotus (*Nelumbo nucifera*), have been a source of inspiration for a wealth of different surface modifications.[1–6] Lotus leaves are self-cleaning, *i.e.*, rain drops remove dirt from the superhydrophobic surfaces, sliding off even at small tilt angles. The leaves have micrometre-sized papillose cells and nanometer-scale patterns in combination with a low-surface-energy wax coating.[7] The hierarchical surface roughness of the leaf is expected to play an important role for the super-hydrophobicity and dirt repellency.[7,8] By a common definition, a surface is superhydrophobic if the contact angle between a water drop and the surface at the solid–liquid–air interface is larger than 150° with a small contact angle hysteresis, and drops readily slide off when the surface is tilted even slightly.[9–11] The above wetting properties are feasible also beyond biology—in addition to the self-cleaning effect, possible applications of superhydrophobic surfaces include prevention of snow and ice adhesion,[12,13] anti-biofouling paints for ships,[14] and low-friction droplet transport in microfluidic devices.[15–17] However, one of the challenges is to prepare the coatings using industrially relevant materials and processes.

For obtaining a superhydrophobic surface, a suitable rough-ness is required, and the hierarchical structure of the roughness plays a significant role.[18] The surfaces mostly have a low surface energy, which can be achieved by using hydrophobic materials or using tailored surface chemistry.[19–21] If these requirements are fulfilled, a water drop applied to the surface can adopt the Cassie wetting state, where air remains trapped in grooves under the drop—a necessary condition for obtaining superhydrophobi-city.[8] For inducing roughness to a surface, a great variety of methods have been previously used, including lithography, crystal growth, aggregating different sized particles together, galvanic replacement with silver,[22] and plasma etching.[11,23] Low surface energies have been achieved either by choosing a hydrophobic substrate for roughening; or alternatively, by chemically post-modifying surfaces using low-surface-energy substances, such as alkylsilanes, perfluorinated silanes, alka-nethiols, or fatty acids.[1]

Cellulose is a widely abundant, sustainable and natural polymer. Native cellulose in plant cell walls forms a hierarchically ordered material, where the individual cellulose polymer chains first crystallize into the cellulose I structure, which results in nanofibrils of *ca.* 3–15 nm in diameter. The nanofibrils pack into larger fibers of several tens of nanometres[24] and finally into macroscopic fibers with micrometre dimensions. The smallest native cellulose nanofibers are usually called nanofibrillated cellulose (NFC) or alternatively microfibrillated cellulose (MFC). NFC can be cleaved

[a] Molecular Materials, Department of Applied Physics, Aalto University (formerly Helsinki University of Technology), FIN-00076, Espoo, Finland. E-mail: robin.ras@aalto.fi
[b] UPM, New Businesses & Development, Tekniikantie 2C, FI-02150, Espoo, Finland
† Electronic supplementary information (ESI) available. See DOI: 10.1039/c2ra00020b

from macroscopic cellulose fibers by several ways to form nanocellulose hydrogels.[25–30] However, the native crystalline form cannot be preserved if a cellulose dissolution step is included in the process. The NFC hydrogels can be processed, *e.g.*, by freeze-drying to form aerogels or by wet extrusion into strong functional fibers.[31–33] Another common processing technique, spray-drying, is widely used, *e.g.*, in pharmaceutical applications employing microcrystalline cellulose and cellulose derivatives.[34,35] This encourages the exploration of spray-drying of NFC hydrogels,[36,37] their available morphologies and properties in the dry state, as well as their use as a template for functionalization.

Previous work on hydrophobic surfaces from native cellulose nanofibers showed droplets strongly adhering to the surface even when tilted at 90°, lacking thus the low contact angle hysteresis that is essential for self-cleaning applications.[38–40] Such surfaces where the droplet remains pinned to the surface also when tilted to 90° or 180° are called high-adhesion superhydrophobic surfaces.[41] Self-cleaning applications require superhydrophobic surfaces to which droplets are not pinned, *i.e.*, having low contact angle hysteresis. Therefore, we were motivated to explore the feasibility of using native cellulose nanofibers for low-adhesion superhydrophobicity.

In this study, we investigate micron-sized porous particles, prepared by spray-drying of NFC hydrogels to allow hierarchical topography. The NFC microparticles, which strongly absorb water due to native surface hydroxyl groups, are hydrophobized using a trichlorosilane surfactant containing a fluorinated alkyl chain and subsequently deposited on a glass plate to form a model surface. We will explore the surface structure and wetting properties, aiming to mimic the hierarchical surface roughness and wetting properties of lotus leaves in a simple way using a model surfactant.

Experimental

Materials

(Tridecafluoro-1,1,2,2-tetrahydrooctyl)trichlorosilane (FOTS) (97%, ABCR, Germany) was used as received, and toluene (99.8%, Aldrich, Germany) was dried using molecular sieves prior to use. Glass slides were first cleaned using water with a detergent (Fairy, Procter & Gamble, UK) and finally rinsed with ethanol. The spray-dried NFC microparticles (UPM-Kymmene Corporation, Finland) were used as received. The particles were prepared by spray-drying UPM Fibril Cellulose hydrogel dispersion at low concentration. The nanofibrillated cellulose was in native form, obtained from bleached birch pulp by mechanical treatment.

Approach A

In the first approach, illustrated in Fig. 1a, a 1% w/w dispersion of NFC microparticles (subsequently denoted as 'microparticles' for simplicity) in ethanol was sprayed with an airbrush onto a glass surface, resulting in a semi-transparent layer. Subsequently, samples were dried in ambient conditions. Finally, the samples were coated with FOTS *via* chemical vapor deposition at 90 °C for 8 h, essentially as described in detail by Jin *et al.*[38]

Approach B

In the second approach, illustrated in Fig. 1b, microparticles were first dispersed in toluene. The particles were observed to
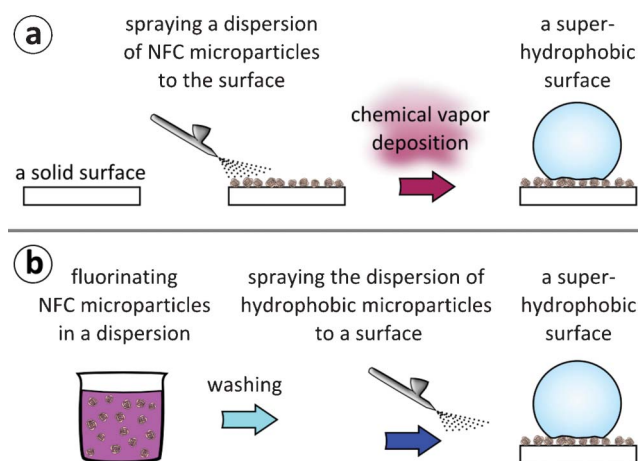

Fig. 1 Two approaches for lotus-leaf mimicking hierarchical topography and wetting properties. **(a)** Approach A: a dispersion of NFC microparticles in ethanol is first sprayed onto a surface. The surface is subsequently coated with FOTS *via* chemical vapor deposition, resulting in a superhydrophobic surface. **(b)** Approach B: a toluene dispersion of NFC microparticles is first reacted with FOTS to fluorinate the microparticles. Subsequently, the microparticle dispersion is washed and finally sprayed onto a substrate, resulting in a superhydrophobic surface.

sediment in a timescale of minutes if not stirred, but the dispersion was stable enough to allow chemical modification. The particles were reacted with FOTS in a dispersion in dry toluene for 3 h under stirring. Subsequently, the microparticles were washed with dry toluene to remove the unreacted FOTS. Finally, the toluene was changed to ethanol. In order to obtain a layer of microparticles, a 1% w/w dispersion of the microparticles in ethanol was sprayed onto a glass surface using an airbrush, and the sample was subsequently dried in ambient conditions.

Characterization

Contact angles were measured using a KSV Instruments CAM 200 optical contact angle measuring device with a software-controlled dispenser. A 25-gauge flat-tipped needle and water purified with a Milli-Q device were used. KSV bundled software was used to fit Young–Laplace curves to images.

To determine the advancing and receding contact angles, a drop of about 2 μl was first applied to a surface using the needle of the dispenser. Subsequently, the needle was lowered so that the tip was near the surface at the back edge of the drop. This way the needle did not disturb the shape of the drop in pictures remarkably, and curve fitting could be performed successfully.

To measure the advancing contact angle, water was added to the drop at the speed of 0.4 ± 0.2 μl s^{-1}, and pictures were taken with 500 ms intervals. After measuring the advancing contact angle, more water was added, resulting in a drop with a volume of at least 20 μl. Subsequently, for measuring the receding contact angle, water was withdrawn at 0.6 ± 0.4 μl s^{-1} and pictures were taken with 500 ms intervals.

A Young–Laplace curve was fitted to each picture, and the contact angle value for a 6.0 μl drop was linearly interpolated using the data range where the width of the drop at the contact line changed at a constant velocity. Usually these volumes ranged from 3 to 10 μl. Drops larger than 10 μl were not used in

calculations, since they were deformed significantly by gravity. When determining the advancing contact angle, the larger of the two contact angles (left and right) was chosen, since the side with the larger contact angle was found to more likely advance. Conversely, when determining the receding contact angle, the smaller of the two angles was used for calculations. The error estimate given with the contact angle values is the standard error of the linear regression.

Scanning Electron Microscopy (SEM) was performed using a JEOL JSM7500FA field emission microscope. Before imaging, a 5-nm layer of Au–Pd was sputtered onto the sample surface.

Results and discussion

The surface morphologies were studied on the model glass substrates prepared using the two approaches shown in Fig. 1, i.e., where the fluorination was made after applying the microparticles on the surface (Approach A) or where the fluorination of the microparticles was made before applying them to the surface (Approach B).

SEM micrographs, presented in Fig. 2, showed surface roughness at several length scales, corresponding quite closely to that of lotus leaves.[7] First, the microparticles on the substrate had irregular shapes and a broad size distribution of 5–20 μm, having roughly the same diameter as the papillose cells on a lotus leaf. Furthermore, the microparticles and lotus papillae have also rather similar distribution on the surface. However, Fig. 2 suggests that the fluorinated microparticles prepared via
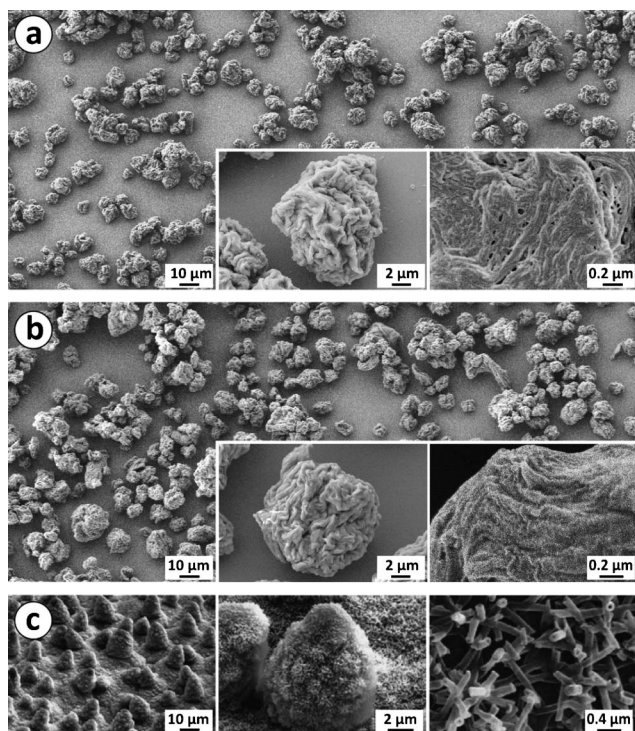

Fig. 2 (a) Surface structures of a sample with spray-dried NFC microparticles by Approach A before fluorination. (b) A sample with fluorinated NFC microparticles, prepared by Approach B. (c) Surface of a lotus leaf with microstructure formed by papillose cells covered with hydrophobic wax tubules (Reproduced by permission of The Royal Society of Chemistry).[7]

Approach B (Fig. 2b) aggregate less and form a denser and more uniform layer than the non-fluorinated microparticles that were prepared by Approach A (Fig. 2a). Second, the spray-dried microparticles have micron-scale roughness similar to the lotus papillae, as shown in Fig. 2. Finally, the NFC nanofibers within the microparticles are aggregated to form sheets in analogy with freeze-dried aerogels.[42,43] The NFC aggregates at the surface have widths of 10–100 nm, corresponding to the width of wax tubules on lotus leaves.[6] Unlike the wax tubules, however, the NFC aggregates do not stick out from the surface, but rather lie parallel with the surface.

Adding the fluorinated spray-dried NFC microparticles to a surface was found to considerably increase the water contact angle, making the surfaces superhydrophobic and enabling water drops to slide off at small tilt angles. Using Approach A, a surface was prepared that had advancing and receding contact angles of 169 ± 4° and 152 ± 4°, respectively, as illustrated in Fig. 3a. Water drops applied to the horizontal surface were observed to slide off readily when the surface was tilted to an angle smaller than five degrees (see Supplementary video 1†). Using Approach B, which consists of first making the particles hydrophobic, and subsequently spraying them onto a substrate, a surface was prepared that had advancing and receding contact angles of 163 ± 3° and 155 ± 3°, respectively. The contact angles are illustrated in Fig. 3b. Also in this case, water drops were observed to slide off the surface at tilt angles smaller than five degrees (see Supplementary video 2†). The current technique utilized for spraying the microparticles to the surface did not allow systematic study of the effect of surface coverage on wetting properties, even though it would be of interest.

The wetting properties were essentially similar in both approaches, even though the glass surface between the microparticles was also fluorinated in Approach A, due to the chemical vapor deposition at the final step, whereas in Approach B, the glass surface was not fluorinated. This indirectly shows that the glass surface between the microparticles
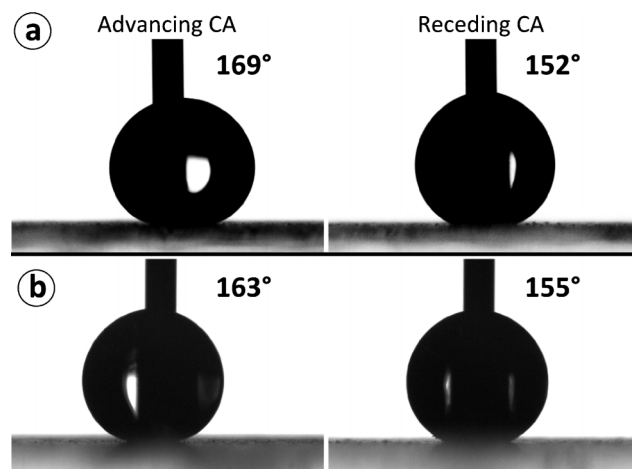

Fig. 3 (a) Contact angles of a surface with NFC microparticles prepared via Approach A, which involves FOTS coating via chemical vapor deposition at the final step. (b) Contact angles of a surface with fluorinated microparticles prepared via Approach B, which involves fluorination of NFC microparticles in a dispersion before applying on the substrate.

does not participate in the wetting properties, which supports the presence of the Cassie wetting state. From a practical point of view, Approach B could have an advantage over Approach A, because Approach B allows a substrate to be made super-hydrophobic in a single coating step.

Even though no adhesive was utilized for binding the particles to the model glass surface, both coatings were relatively stable upon droplet impacts. Both surfaces were found to remain hydrophobic enough for water droplets to bounce off the surface without residue after more than 100 impacts of falling droplets to the same spot on the surface, as shown by Supplementary video 3 (Approach A) and Supplementary video 4 (Approach B).† Still the coating could be damaged by mechanical abrasion. We foresee that the stability of the coating could be considerably improved by employing an adhesive for binding the particles to the surface.

The Cassie wetting state with its thin layer of trapped air (called the plastron) can also be directly shown. Total reflection of light is observed at the air–water interface at the surface of a sample immersed in water when viewed from an angle larger than the critical angle of total internal reflection. Similar demonstration of the plastron was carried out by Larmour et al. for superhydrophobic metal surfaces.[22] In order to make observation of the reflection easier, orange paper was placed at the backside of the sample. The plastron at the surface of a sample immersed in water is shown in Fig. 4a. Together with the large contact angles, this observation implies that the surface is

superhydrophobic. In addition to having superhydrophobic properties, the NFC microparticle coating is semi-transparent, as shown in Fig. 4b. The microparticles are large enough to scatter light, but since they do not entirely cover the surface, light is transmitted through the coating.

It was also observed that if a water drop rolls on top of an excessive amount of hydrophobic powder of NFC microparticles prepared by Approach B, the cellulose particles will cover the drop surface forming liquid marbles (for liquid marbles and their possible applications, the reader is recommended to see, e.g., a review by Aussillous and Quéré).[44] Fig. 4c shows two such liquid marbles on a hydrophilic glass surface. The cellulose microparticles effectively prevent the water drop from wetting the glass surface.

Conclusions

Two approaches were employed for preparing superhydrophobic surfaces using microparticles of spray-dried native cellulose nanofibers, i.e., nanofibrillated cellulose (NFC). The first approach consisted of applying the microparticles to a substrate, followed by a gas phase coating with a fluorine-containing trichlorosilane surfactant via chemical vapor deposition, and the second approach included hydrophobization of the microparticles in a solution with the fluorinated trichlorosilane surfactant, followed by applying the particles to the substrate. Both methods resulted in superhydrophobic surfaces, as determined by contact angle measurements and observation of reflection when immersed in water. Importantly, sliding angles of only a few degrees were achieved using both approaches, which potentially enables self-cleaning applications. In addition, liquid marbles were prepared using hydrophobic cellulose particles prepared by the second approach. The surface pattern achieved by depositing the spray-dried NFC microparticles on surfaces was observed to have hierarchical roughness qualitatively similar to lotus leaves. Furthermore, spray-dried NFC microparticles are particularly attractive for preparing superhydrophobic surfaces, since cellulose is a cheap, natural product available in large amounts and spray-drying of cellulose nanofibers is an industrially feasible process.

Acknowledgements

References

1 X. Zhang, F. Shi, N. Jia, J. Yugui and W. Zhiqiang, J. Mater. Chem., 2008, 18, 621–633.
2 K. Koch, B. Bhushan and W. Barthlott, Prog. Mater. Sci., 2009, 54, 137–178.
3 I. P. Parkin and R. G. Palgrave, J. Mater. Chem., 2005, 15, 1689–1695.
4 R. Blossey, Nat. Mater., 2003, 2, 301–306.
5 Q. Cheng, M. Li, Y. Zheng, B. Su, S. Wang and L. Jiang, Soft Matter, 2011, 7, 5948–5951.
6 T. Verho, C. Bower, P. Andrew, S. Franssila, O. Ikkala and R. H. A. Ras, Adv. Mater., 2011, 23, 673–678.
7 K. Koch, B. Bhushan, Y. C. Jung and W. Barthlott, Soft Matter, 2009, 5, 1386–1393.
8 T.-S. Wong and C.-M. Ho, Langmuir, 2009, 25, 12851–12854.
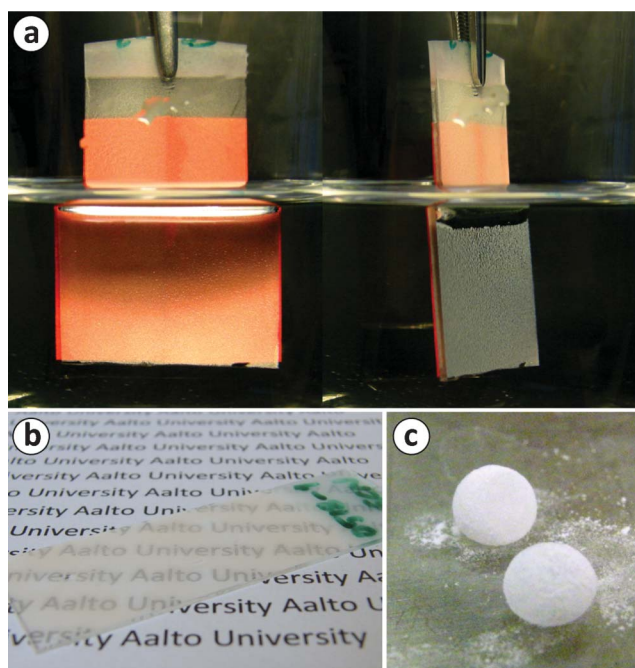9 C. Dorrer and J. Rühe, Soft Matter, 2009, 5, 51–61.

Fig. 4 (a) A glass slide of fluorinated NFC microparticles, prepared using Approach A, immersed in water. When viewed beyond the critical angle, a total internal reflection can be observed, implying the presence of the plastron, and thus, superhydrophobicity. Orange paper was attached at the backside of the sample in order to facilitate observation of the reflection. (b) A photograph demonstrating the semi-transparency of a superhydrophobic sample prepared using Approach A. (c) Liquid marbles, i.e., water drops coated with the hydrophobic microparticles, on a hydrophilic glass.

10 M. Nosonovsky and B. Bhushan, *J. Phys.: Condens. Matter*, 2008, **20**, 395005.

11 P. Roach, N. J. Shirtcliffe and M. I. Newton, *Soft Matter*, 2008, **4**, 224–240.

12 T. Kako, A. Nakajima, H. Irie, Z. Kato, K. Uematsu, T. Watanabe and K. Hashimoto, *Journal of Materials Science*, 2004, **39**, 547–555.

13 S. A. Kulinich and M. Farzaneh, *Appl. Surf. Sci.*, 2009, **255**, 8153–8157.

14 J. Genzer and K. Efimenko, *Biofouling: The Journal of Bioadhesion and Biofilm Research*, 2006, **22**, 339–360.

15 S. M. Kim, S. H. Lee and K. Y. Suh, *Lab Chip*, 2008, **8**, 1015–1023.

16 P. Joseph, C. Cottin-Bizonne, J. M. Benoît, C. Ybert, C. Journet, P. Tabeling and L. Bocquet, *Phys. Rev. Lett.*, 2006, **97**, 156–104.

17 H. Mertaniemi, V. Jokinen, L. Sainiemi, S. Franssila, A. Marmur, O. Ikkala and R. H. A. Ras, *Adv. Mater.*, 2011, **23**, 2911–2914.

18 L. F. Cheow, L. Yobas and D.-L. Kwong, *Appl. Phys. Lett.*, 2007, **90**, 054107.

19 L. Gao and T. J. McCarthy, *Langmuir*, 2006, **22**, 2966–2967.

20 M. Nosonovsky, *Langmuir*, 2007, **23**, 3157–3161.

21 K. Liu, X. Yao and L. Jiang, *Chem. Soc. Rev.*, 2010, **39**, 3240–3255.

22 I. A. Larmour, S. E. J. Bell and G. C. Saunders, *Angew. Chem., Int. Ed.*, 2007, **46**, 1710–1712.

23 V. Zorba, E. Stratakis, M. Barberoglou, E. Spanakis, P. Tzanetakis, S. H. Anastasiadis and C. Fotakis, *Adv. Mater.*, 2008, **20**, 4049–4054.

24 S. Eichhorn, A. Dufresne, M. Aranguren, N. Marcovich, J. Capadona, S. Rowan, C. Weder, W. Thielemans, M. Roman, S. Renneckar, W. Gindl, S. Veigel, J. Keckes, H. Yano, K. Abe, M. Nogi, A. Nakagaito, A. Mangalam, J. Simonsen, A. Benight, A. Bismarck, L. Berglund and T. Peijs, *J. Mater. Sci.*, 2010, **45**, 1–33.

25 A. F. Turbak, F. W. Snyder and K. R. Sandberg, *J. Appl. Polym. Sci.: Appl. Polym. Symp.*, 1983, **37**, 815–827.

26 D. Klemm, F. Kramer, S. Moritz, T. Lindström, M. Ankerfors, D. Gray and A. Dorris, *Angew. Chem., Int. Ed.*, 2011, **50**, 5438–5466.

27 K. Abe, S. Iwamoto and H. Yano, *Biomacromolecules*, 2007, **8**, 3276–3278.

28 T. Saito, S. Kimura, Y. Nishiyama and A. Isogai, *Biomacromolecules*, 2007, **8**, 2485–2491.

29 M. Pääkkö, M. Ankerfors, H. Kosonen, A. Nykänen, S. Ahola, M. Österberg, J. Ruokolainen, J. Laine, P. T. Larsson, O. Ikkala and T. Lindström, *Biomacromolecules*, 2007, **8**, 1934–1941.

30 M. Henriksson, G. Henriksson, L. A. Berglund and T. Lindström, *Eur. Polym. J.*, 2007, **43**, 3434–3441.

31 O. Ikkala, R. H. A. Ras, N. Houbenov, J. Ruokolainen, M. Pääkkö, J. Laine, M. Leskelä, L. A. Berglund, T. Lindström, G. ten Brinke, H. Iatrou, N. Hadjichristidis and C. F. J. Faul, *Faraday Discuss.*, 2009, **143**, 95–107.

32 S. Iwamoto, A. Isogai and T. Iwata, *Biomacromolecules*, 2011, **12**, 831–836.

33 A. Walther, J. V. I. Timonen, I. Díez, A. Laukkanen and O. Ikkala, *Adv. Mater.*, 2011, **23**, 2924–2928.

34 R. Vehring, *Pharm. Res.*, 2008, **25**, 999–1022.

35 Q. Cao, H.-s. Kim, N. Pimparkar, J. P. Kulkarni, C. Wang, M. Shim, K. Roy, M. A. Alam and J. A. Rogers, *Nature*, 2008, **454**, 495–500.

36 R. Kolakovic, L. Peltonen, T. Laaksonen, K. Putkisto, A. Laukkanen and J. Hirvonen, *AAPS PharmSciTech*, 2011, **12**, 1366–1373.

37 J. Vartiainen, T. Pöhler, K. Sirola, L. Pylkkänen, H. Alenius, J. Hokkinen, U. Tapper, P. Lahtinen, A. Kapanen, K. Putkisto, P. Hiekkataipale, P. Eronen, J. Ruokolainen and A. Laukkanen, *Cellulose*, 2011, **18**, 775–786.

38 H. Jin, M. Kettunen, A. Laiho, H. Pynnönen, J. Paltakari, A. Marmur, O. Ikkala and R. H. A. Ras, *Langmuir*, 2011, **27**, 1930–1934.

39 M. Kettunen, R. J. Silvennoinen, N. Houbenov, A. Nykänen, J. Ruokolainen, J. Sainio, V. Pore, M. Kemell, M. Ankerfors, T. Lindström, M. Ritala, R. H. A. Ras and O. Ikkala, *Adv. Funct. Mater.*, 2010, **21**, 510–517.

40 C. Aulin, J. Netrval, L. Wågberg and T. Lindström, *Soft Matter*, 2010, **6**, 3298–3305.

41 M. Liu, Y. Zheng, J. Zhai and L. Jiang, *Acc. Chem. Res.*, 2010, **43**, 368–377.

42 M. Pääkkö, J. Vapaavuori, R. Silvennoinen, H. Kosonen, M. Ankerfors, T. Lindström, L. A. Berglund and O. Ikkala, *Soft Matter*, 2008, **4**, 2492–2499.

43 H. Sehaqui, M. Salajkova, Q. Zhou and L. A. Berglund, *Soft Matter*, 2010, **6**, 1824–1832.

44 P. Aussillous and D. Quéré, *Proc. R. Soc. London, Ser. A*, 2006, **462**, 973–999.